

# OBSERVED SPATIAL PROPERTIES OF THE SOLAR EIGENFUNCTIONS AND THE IMPLICATIONS FOR THE EXISTENCE OF RESOLVED MULTIPLETS

Thomas P. Caudell  
SCLERA, Department of Physics  
University of Arizona, Tucson, AZ, USA

Henry A. Hill  
Professor, Department of Physics  
University of Arizona, Tucson, AZ, USA

and

Randall J. Bos  
SCLERA, Department of Physics  
University of Arizona, Tucson, AZ, USA

## INTRODUCTION

Solar oscillations are manifested in the solar atmosphere as spatial and temporal perturbations in the local thermodynamical and mechanical properties. When measuring the solar radius/diameter, these perturbations enter the observation through changes in the radiative source function and opacity at the extreme limb. When compared to the disk center, the observable portion of these perturbations is changed in spatial character by projection effects and oblique optical-depth geometry. The time-varying solar radius signal at SCLERA<sup>1</sup> is produced by an edge definition sensitive to the resultant changes in the spatial shape of the limb intensity profile. The object of this study is to interlace theory and observation in an attempt to further determine the shape and properties of the limb signals which display these global solar oscillations. The following sections review the observations and discuss the methods and results of this study.

---

<sup>1</sup>SCLERA is an acronym for the Santa Catalina Laboratory for Experimental Relativity by Astrometry jointly operated by the University of Arizona and Wesleyan University.

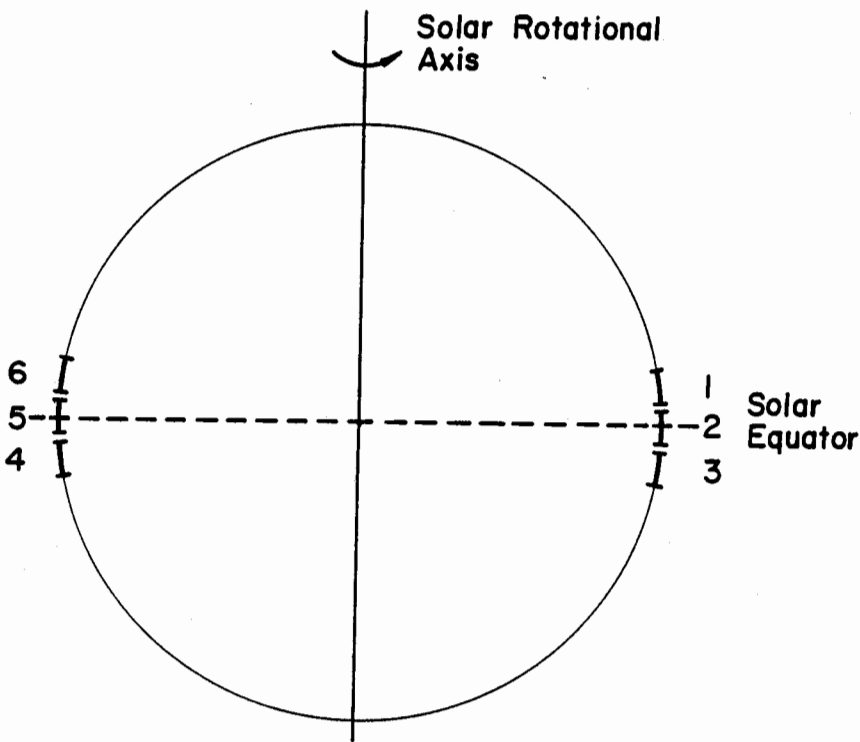


Fig. 1. The detector geometry for the 1979 SCLERA data set. The numbers label the locations of the six limb intensity photodetectors.

#### CHARACTERISTICS OF THE 1979 SCLERA DATA

The data considered in this analysis were collected in the summer of 1979 using the SCLERA instrument. Both the instrument and the details of the data analysis have been described in other works (Stebbins 1975, Bos 1982); therefore, only a brief summary of the salient points will be given here.

Over a period of 41 days, time strings were recorded of intensity profiles at the extreme limb; the measurements were taken at six position angles near the solar equator. The detector geometry is shown in Figure 1. Off-line, the finite Fourier transform definition (FFTD) was applied twice to each profile with window sizes of  $27^{\circ}2$  and  $6^{\circ}8$  [see Hill, Stebbins and Oleson (1975) for a detailed description of the FFTD]. Differences were then taken between the two defined radii to form six time strings of radius functionals primarily sensitive to changes in limb profile shape. Finally, linked baseline temporal Fourier transforms were performed on the six time strings over the entire observing period.

By linearly combining the six transforms, different symmetry conditions can be enforced, controlling the parity of the spatial part of the oscillation about the solar equator or the north-south line. Mathematically, the solutions which describe an oscillation are products of a radial eigenfunction and a spherical harmonic, with order numbers  $n$  and  $(\ell, m)$  respectively. Setting the parity amounts to assigning the  $\ell$  and  $m$  order numbers to be even or odd. This property somewhat reduces the spectral peak density in a given linear combination and aids in the identification of modes.

Two linear combinations are used in this analysis;  $F_1$  and  $F_2$  refer to the sum and difference, respectively, of the two diametrically opposite groups of limb signals. Each group consists of the sum of three individual radius functionals. Since the Fourier transform is a linear operator, combining the individual transforms is equivalent to combining the radius functional time strings; these procedures therefore may be used interchangeably. The properties of the observed signal combinations may be quantified by first assuming the spatial and temporal form of the intensity perturbation at the limb to be

$$I'_{\ell m}(u, t) = I'_{\ell 0}(u) \cdot \exp \left\{ i (\phi_m + m\phi + \omega t) \right\} \quad (1)$$

where  $u$  is the distance from the nominal disk edge,  $I'_{\ell 0}(u)$  is the  $m = 0$ ,  $t = 0$  radial perturbation,  $\phi$  is the standard angle in a spherical coordinate system,  $\phi_m$  is the initial phase angle of the particular state in the  $\phi$  direction, and  $\omega$  is the temporal angular frequency. We define the two combinations to be

$$\begin{aligned} F_1 &= \text{FFTD} \left[ f_1(\ell, m, \phi_m, \phi, \omega, t) \right] \\ F_2 &= \text{FFTD} \left[ f_2(\ell, m, \phi_m, \phi, \omega, t) \right] \end{aligned} \quad (2)$$

where

$$\begin{aligned} f_1 &= \left[ \frac{1 + (-1)^{\ell+m}}{2} \right] \left[ \text{Re } I'_{\ell 0} \cos(\phi_m + \omega t) - \text{Im } I'_{\ell 0} \sin(\phi_m + \omega t) \right] \\ &\quad \left\{ (-1)^{m/2} \left[ \frac{1 + (-1)^m}{2} \right] \cos m \left( \frac{\pi}{2} - \phi_+ \right) \right. \\ &\quad \left. + (-1)^{(m-1)/2} \left[ \frac{1 - (-1)^m}{2} \right] \sin m \left( \frac{\pi}{2} - \phi_+ \right) \right\} \end{aligned} \quad (3)$$

$$\begin{aligned}
f_2 = & \left[ \frac{1 + (-1)^{\ell+m}}{2} \right] \left[ \text{Re } I'_{\ell_0} \sin(\phi_m + \omega t) + \text{Im } I'_{\ell_0} \cos(\phi_m + \omega t) \right] \\
& \left\{ (-1)^{m/2} \left[ \frac{1 + (-1)^m}{2} \right] \sin m \left( \frac{\pi}{2} - \phi_+ \right) \right. \\
& \left. - (-1)^{(m-1)/2} \left[ \frac{1 - (-1)^m}{2} \right] \cos m \left( \frac{\pi}{2} - \phi_+ \right) \right\}, \tag{3}
\end{aligned}$$

and  $\phi_+$  is  $\phi$  measured positively from the disk edge toward the center. The notation FFTD [ ] symbolizes the conversion of changes in the limb darkening function into radius functionals defined as differences between two FFTD edges;  $F_1$  and  $F_2$  are in units of distance.

Specific information about  $I'_{\ell m}$  can be obtained by taking a ratio between these two quantities at the assigned temporal frequency for a given mode of oscillation. This procedure allows the testing of the spherical harmonic representation of the eigenfunction, particularly the  $e^{im\phi}$  portion. An additional consistency test of the symmetry properties may thus be made. Measurement of the radial shape and phase of the intensity perturbation is also possible. Further, by taking the ratio of  $F_1$  and  $F_2$ , cancellation is effected of differences in modal amplitude due either to excitation or spatial filtering of the  $P_{\ell m}(\theta, \phi)$ ; comparison between modes is then possible. In practice, extraction of the above information requires that the ratio be studied as a function of azimuthal order number  $m$ . This method implicitly uses the frequency splitting of the states into resolved multiplets.

In the work of Hill and Bos (1984), a series of 32 rotationally split multiplets has been identified; these states vary in degree  $\ell$  from 2 to 22 and in nodal index  $n$  from 1 to 3. The frequencies range between 450 and 800  $\mu\text{Hz}$ , implying the  $p$ -mode assignment. At the time of this writing, four of these multiplets were available for ratio analysis (see Table 1). Figures 2 and 3 display separate averages of the real and imaginary parts of the ratio, with negative  $m$  states having been reflected through the origin and averaged with positive  $m$ . Given the size of the error bars, significant structure is present in both the real and imaginary portions. The object of this analysis is to invert the structure evident in this data and extract the properties of the source intensity perturbation.

TABLE 1. Four Multiplets Used in Inversion Analysis

$P_{n,1} : P_{1,10} P_{1,14} P_{1,22} P_{3,4}$

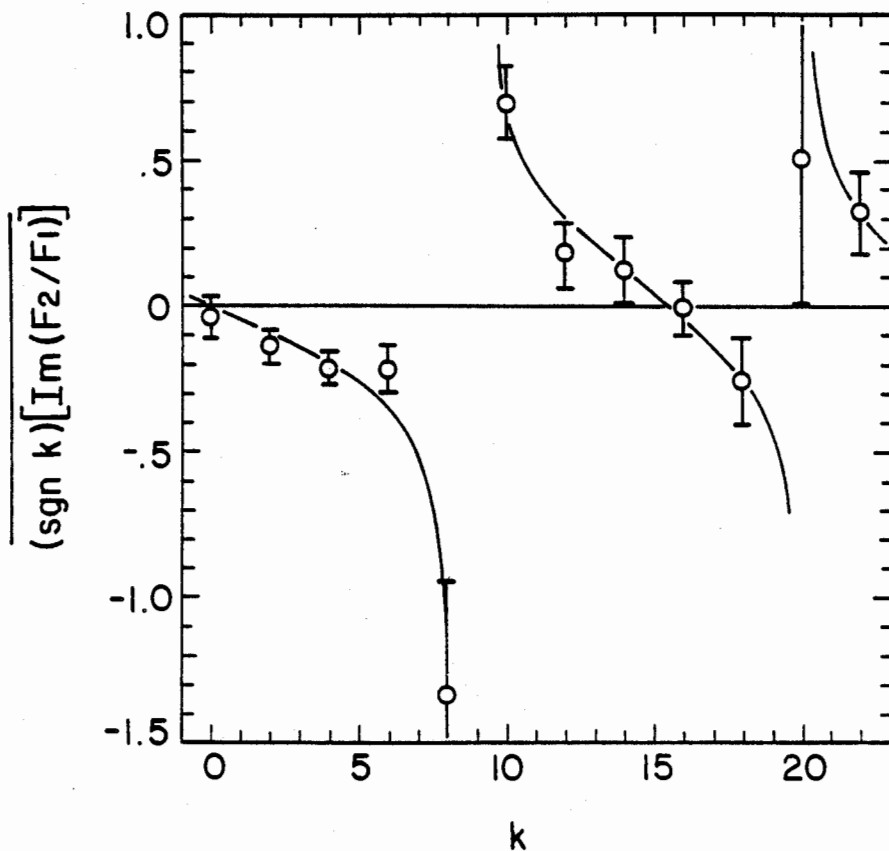


Figure 2. Imaginary part of ratio  $(F_2/F_1)$  averaged in  $m$  for four multiplets. The smooth curve is not a fit.

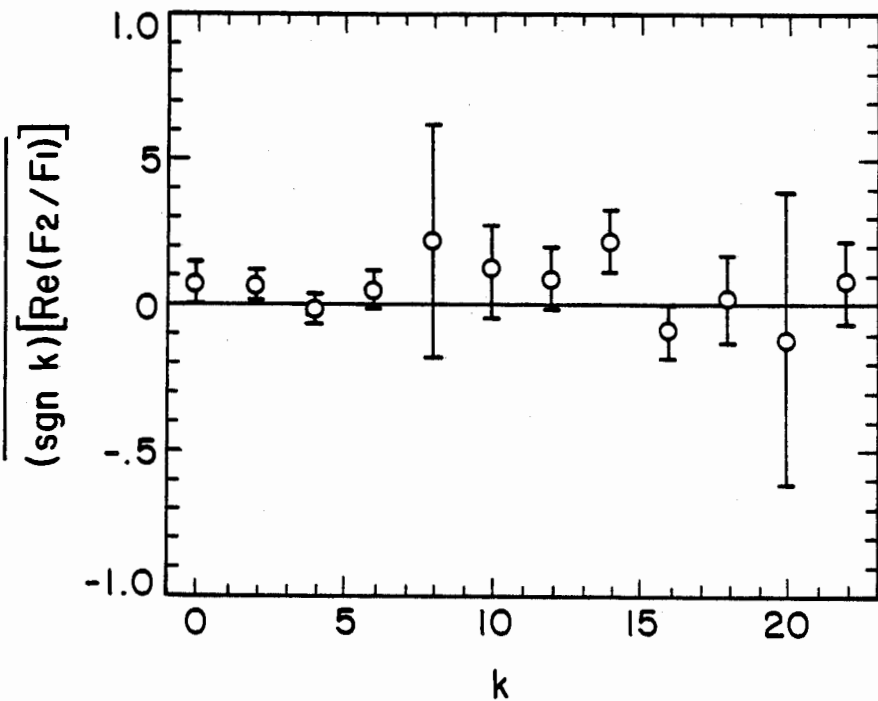


Figure 3. Real part of ratio  $(F_2/F_1)$  averaged in  $m$  for four multiplets.

#### RESULTS OF THE INVERSION TECHNIQUE

A simple representation is needed for the initial inversion. The present work assumes that the intensity perturbation is all of one spatial phase; this phase is also chosen so that  $I'_\ell(u)$  is real. The radial form of  $I'_\ell(u)$  is expanded in a generalized <sup>$\ell_0$</sup>  power series where a minimum number <sup>$\ell_0$</sup>  of individual components are selected to give the best fit to the ratio data. Hence,

$$I'_{\ell m}(u) = \left( \sum_{\alpha} a_{\alpha} g_{\alpha}(u) \right) \left( \cos m\phi(u) + i \sin m\phi(u) \right). \quad (4)$$

The  $a_{\alpha}$  will be determined by the fitting procedure, the  $g_{\alpha}(u)$  are members of a subset of all monomials of the form

$$u^{\pm j/k} \quad (\text{i.e., } u, u^{\pm}, u^{-1}, u^{-1/2}, \text{ etc.}), \quad (5)$$

$\alpha$  is the pointer into this subset, and

$$\phi(u) = \cos^{-1} \left( 1 + \frac{u}{R_{\odot}} \right)$$

where  $R_{\odot}$  is the radius of the sun. Again,  $u$  is a linear distance measure on the solar disk, with the origin at the nominal edge and defined positively outwards. Note that, although the coefficients  $a_{\alpha}$  will generally be complex, they are real in this simplification.

Applying the FFTD operation to the individual components of this representation, we define two new functions

$$\begin{aligned} \psi_{\alpha}(m) &= \text{FFTD} \left[ g_{\alpha}(u) \cdot \sin m\phi(u) \right] \\ \text{and} \\ \beta_{\alpha}(m) &= \text{FFTD} \left[ g_{\alpha}(u) \cdot \cos m\phi(u) \right] \end{aligned} \quad (6)$$

where  $\psi_{\alpha}(m)$  and  $\beta_{\alpha}(m)$  are units of distance and  $u$  has been removed by integration in the FFTD procedure. Equation (2) shows the relationship between  $F_1$  and  $\psi_{\alpha}(m)$  and between  $F_2$  and  $\beta_{\alpha}(m)$ . The form of the ratio discussed earlier is now defined to be

$$R(m) = F_2/F_1 = \frac{\sum_{\alpha} a_{\alpha} \psi_{\alpha}(m)}{\sum_{\alpha} a_{\alpha} \beta_{\alpha}(m)}, \quad (7)$$

where the temporal dependence and amplitude cancel. A fitting procedure must now be applied to determine the  $a_{\alpha}$ . Clearly, without loss of generality we may set  $a_0 = 1$  independent of the form of  $g_{\alpha}(u)$ . Several fitting procedures have been developed to handle the general problem of complex coefficients. A simple approach was chosen here to illustrate the sensitivity of this method. In future work, a general technique will be used to invert the more complete set of ratio data including all 32 multiplets.

In the simple approach, the subset of  $g_{\alpha}(u)$  used is  $u^0, u^{+1}, u^{+1/2}$  necessitating the determination of only two free parameters,  $a_1$  and  $a_2$ . The coefficient  $a_0$  is set to unity as discussed above. Requiring  $R(m)$  to be infinite at  $m = 9$  and zero at  $m = 16$ , values of  $a_1 = -0.0709$  and  $a_2 = -0.5664$  are obtained. A continuous evaluation of  $R(m)$  is given in Figure 4, and Figure 5 shows a reconstruction of  $I'_{\ell_0}(u)$  for this model. For comparison,  $R(m)$  is calculated and plotted for a constant  $I'_{\ell_0}(u)$  (i.e.,  $a_0 = 1, a_1 = 0 = a_2$ ); these results appear in Figure 6.

Comparing the results for the simple model to the ratios averaged over four multiplets in Figure 3, we see that the general structures are quite similar, notwithstanding the difference in overall magnitude. Conversely, the data and Model 2 show little similarity.

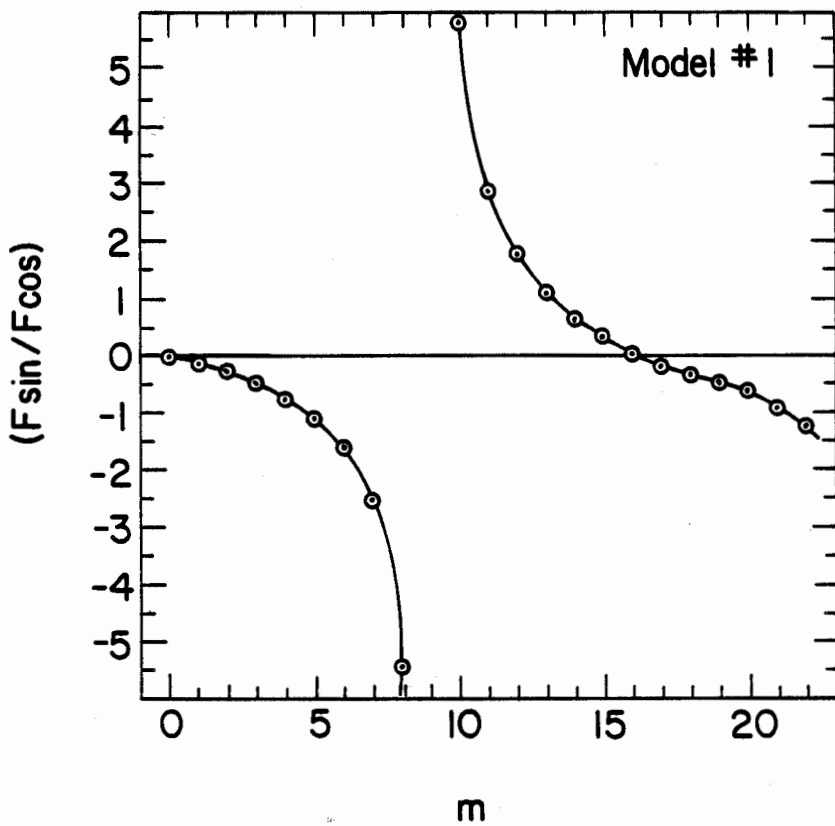


Figure 4. Resultant ratio curve when a singularity is imposed at  $m = 9$  and a zero at  $m = 6$ .

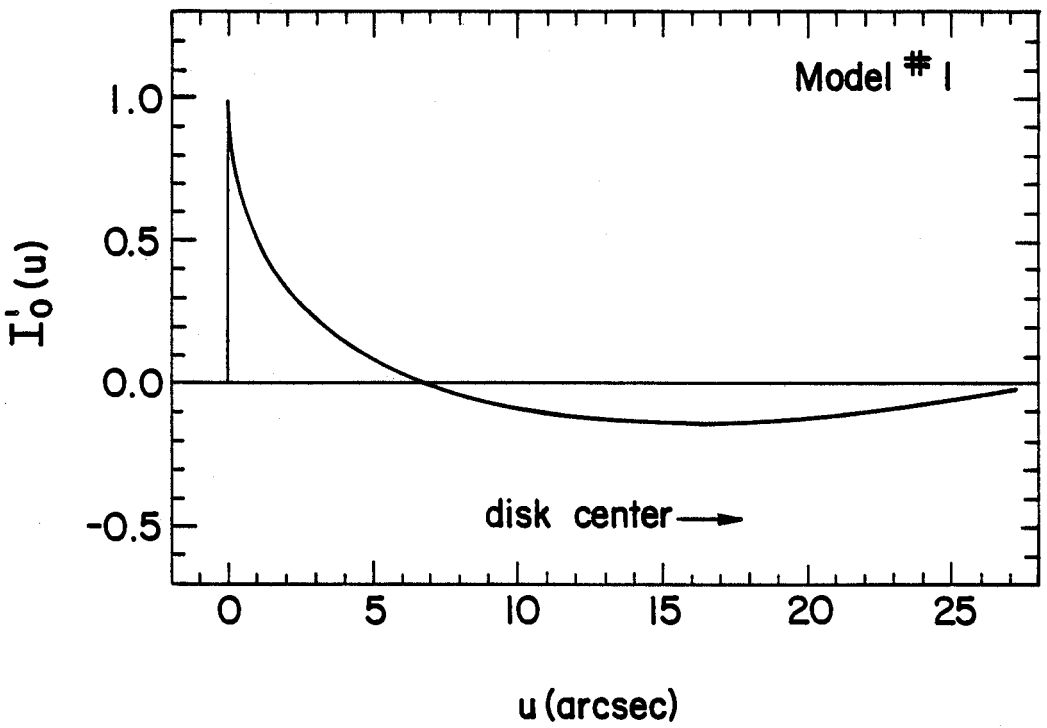


Figure 5. Reconstruction of intensity perturbation fit which gives ratios in qualitative agreement with data.

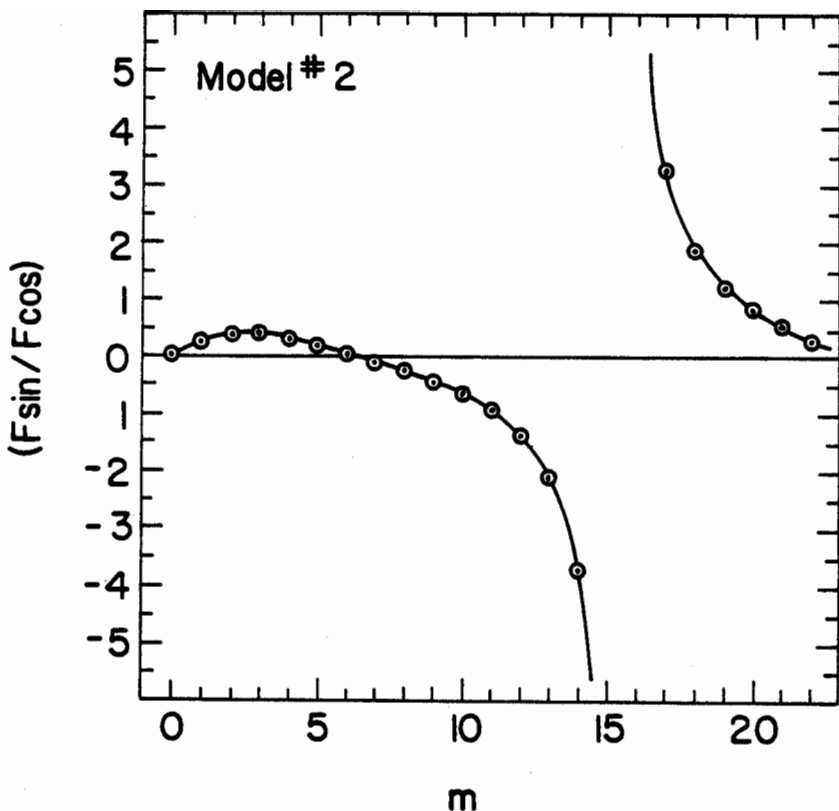


Figure 6. Resultant ratio curve for a spatially constant  $I'_{l_0}(m)$ .

### CONCLUSION

The simple example presented above serves two purposes. First, it illustrates the potential sensitivity with which radiative processes in the solar atmosphere may be probed. A comparison of Figures 4 and 6 graphically demonstrates this aspect. Second, the shape of the intensity perturbation at the extreme limb must be peaked in the outermost layers of the solar atmosphere, a result consistent with previous work at SCLERA (Hill and Caudell 1979; Knapp et al. 1980). The model used in this work is a simplified one and was applied only to a subset of the data; therefore, the present results must be considered preliminary.

This work was partially supported by the Air Force Office of Scientific Research and the National Science Foundation Division of Atmospheric Sciences.

## REFERENCES

1. Bos, R. J., Ph.D. Thesis, University of Arizona (1982).
2. Hill, H. A. and Bos, R. J., In preparation (1984).
3. Hill, H. A. and Caudell, T. P., Mon. Not. R. Astro. Soc. 186, 327 (1979).
4. Hill, H. A., Stebbins, R. T. and Oleson, J. R., Ap. J. 200, 484 (1975).
5. Knapp, J., Hill, H. A. and Caudell, T. P., Nonradial and Nonlinear Stellar Pulsation, Lecture Notes in Physics No. 125 (Springer - Verlag, Berlin, 1980).
6. Stebbins, R. T., Ph.D. Thesis, University of Colorado (1975).